

# UC Berkeley

## UC Berkeley Previously Published Works

### Title

Role for Visual Experience in the Development of Direction-Selective Circuits

### Permalink

<https://escholarship.org/uc/item/4549403b>

### Journal

Current Biology, 26(10)

### ISSN

0960-9822

### Authors

Bos, Rémi  
Gainer, Christian  
Feller, Marla B

### Publication Date

2016-05-01

### DOI

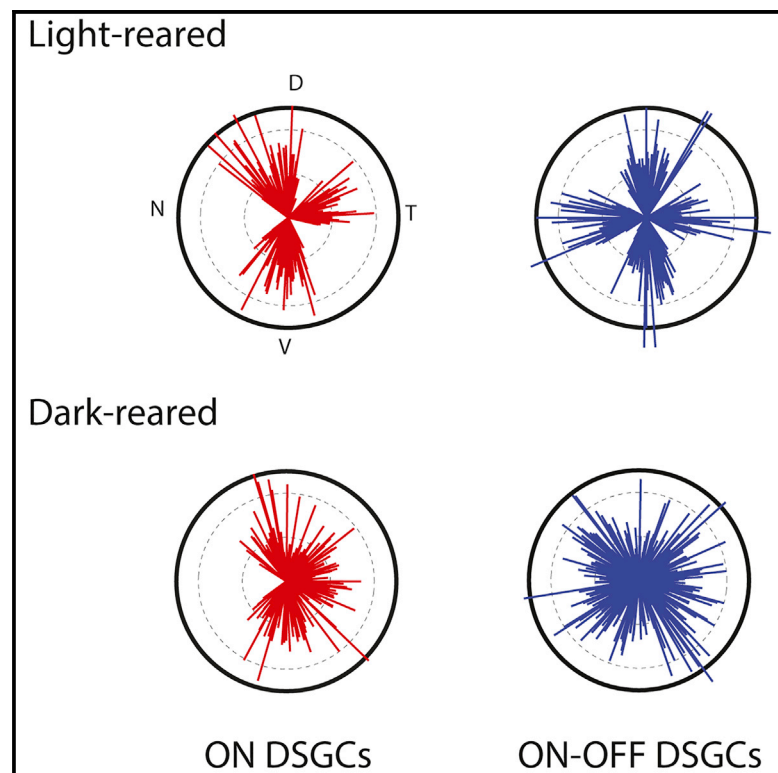
10.1016/j.cub.2016.03.073

Peer reviewed

# Current Biology

## Role for Visual Experience in the Development of Direction-Selective Circuits

### Graphical Abstract



### Authors

Rémi Bos, Christian Gainer,  
Marla B. Feller

### Correspondence

mfeller@berkeley.edu

### In Brief

Bos et al. show that, unlike in adults, at eye-opening the preferred directions of both ON and ON-OFF DSGCs are diffusely distributed and that visual deprivation prevents clustering of these preferred directions along the cardinal directions. Their findings indicate that visual experience plays a critical role in shaping response tuning in the retina.

### Highlights

- Two-photon calcium imaging was used to identify DSGCs across development
- At eye-opening, preferred directions of both DSGC types are diffusely distributed
- Visual deprivation prevents the clustering of preferred directions
- Vision-dependent clustering along cardinal axes occurs via realignment rather than refinement



# Role for Visual Experience in the Development of Direction-Selective Circuits

Rémi Bos,<sup>1,4</sup> Christian Gainer,<sup>2</sup> and Marla B. Feller<sup>1,3,\*</sup><sup>1</sup>Department of Molecular and Cell Biology<sup>2</sup>School of Optometry<sup>3</sup>Helen Wills Neuroscience Institute

University of California, Berkeley, Berkeley, CA 94720-3200, USA

<sup>4</sup>Present address: Institut de Neurosciences de la Timone (UMR 7289), Aix-Marseille Université and CNRS, 13005 Marseille, France\*Correspondence: [mfeller@berkeley.edu](mailto:mfeller@berkeley.edu)<http://dx.doi.org/10.1016/j.cub.2016.03.073>

## SUMMARY

Visually guided behavior can depend critically on detecting the direction of object movement. This computation is first performed in the retina where direction is encoded by direction-selective ganglion cells (DSGCs) that respond strongly to an object moving in the preferred direction and weakly to an object moving in the opposite, or null, direction (reviewed in [1]). DSGCs come in multiple types that are classified based on their morphologies, response properties, and targets in the brain. This study focuses on two types—ON and ON-OFF DSGCs. Though animals can sense motion in all directions, the preferred directions of DSGCs in adult retina cluster along distinct directions that we refer to as the cardinal axes. ON DSGCs have three cardinal axes—temporal, ventral, and dorsonasal—while ON-OFF DSGCs have four—nasal, temporal, dorsal, and ventral. How these preferred directions emerge during development is still not understood. Several studies have demonstrated that ON [2] and ON-OFF DSGCs are well tuned at eye-opening, and even a few days prior to eye-opening, in rabbits [3], rats [4], and mice [5–8], suggesting that visual experience is not required to produce direction-selective tuning. However, here we show that at eye-opening the preferred directions of both ON and ON-OFF DSGCs are diffusely distributed and that visual deprivation prevents the preferred directions from clustering along the cardinal axes. Our findings indicate a critical role for visual experience in shaping responses in the retina.

## RESULTS

### Clustering of Direction-Selective Ganglion Cell Preferred Directions along Cardinal Axes after Eye-Opening Requires Visual Experience

We used two-photon calcium imaging to study the development of direction-selective ganglion cells (DSGC) populations in

mouse retina. This imaging technique has proved to be quite powerful in characterizing the receptive field properties of retinal ganglion cells [9–12]. We loaded retinas of wild-type (WT) mice near eye-opening (P13–P14) and in adulthood (>P30) with the calcium dye Oregon green 488 BAPTA-1 hexapotassium salt (OGB-1) via electroporation, thus uniformly labeling the ganglion cell layer (Figure 1A; see the Supplemental Information). Ventral portions of the retina were stimulated with light centered at 385 nm to maximally activate UV cones [13, 14] while minimizing crosstalk with the imaging detectors (Figure S1). This approach allowed us to record from all DSGC subtypes within a single field of view (~40,000  $\mu\text{m}^2$ ).

To identify DSGCs, we first used full-field UV-light flashes to classify cells as ON, OFF, or ON-OFF retinal ganglion cells (RGCs) (Figure S1; Table S1). We found that around 80% of the cells in the ganglion cell layer of young and adult retinas responded to light flashes with changes in fluorescence (Table S1), similar to the RGC percentages reported in previous studies [9, 11, 12]. In addition, over development we observed a decrease in the percentage of ON-OFF RGCs (28.03% at P13–P14 to 20.84% in adult) (Table S1) [15].

Second, we used light bars on a dark background drifting in eight directions to identify and classify ON and ON-OFF DSGCs. In adult (>P30) and young (P13–P14) retinas, both ON and ON-OFF DSGCs were readily distinguishable (Figure 1B; Table S1; Supplemental Information) and DSGCs in the same field of view displayed different preferred directions (Figure 1C; Figure S1). For both ages, ON and ON-OFF DSGCs displayed stable preferred directions in response to two consecutive imaging sessions (Figure 1D). Finally, DSGCs had significantly reduced tuning in the presence of the GABA<sub>A</sub> receptor blocker, gabazine (5–10  $\mu\text{M}$ ;  $n = 56$  cells from four retinas) (Figures 1E–1G). These effects were observed both in young and adult retinas, confirming that the asymmetric inhibition that generates the directional tuning is established and functional at early developmental stages in both DSGC types [7, 16, 17]. Together, these experiments indicate that we can reliably record from stable populations of ON and ON-OFF DSGCs.

We next investigated the distribution of preferred directions of these DSGCs in adult and at eye-opening. In adult retinas, we found that the preferred directions of ON DSGCs clustered along three cardinal axes while the preferred directions of ON-OFF DSGCs clustered along four axes [1, 18, 19]. However, at eye-opening (P13–P14), the preferred directions of both ON and

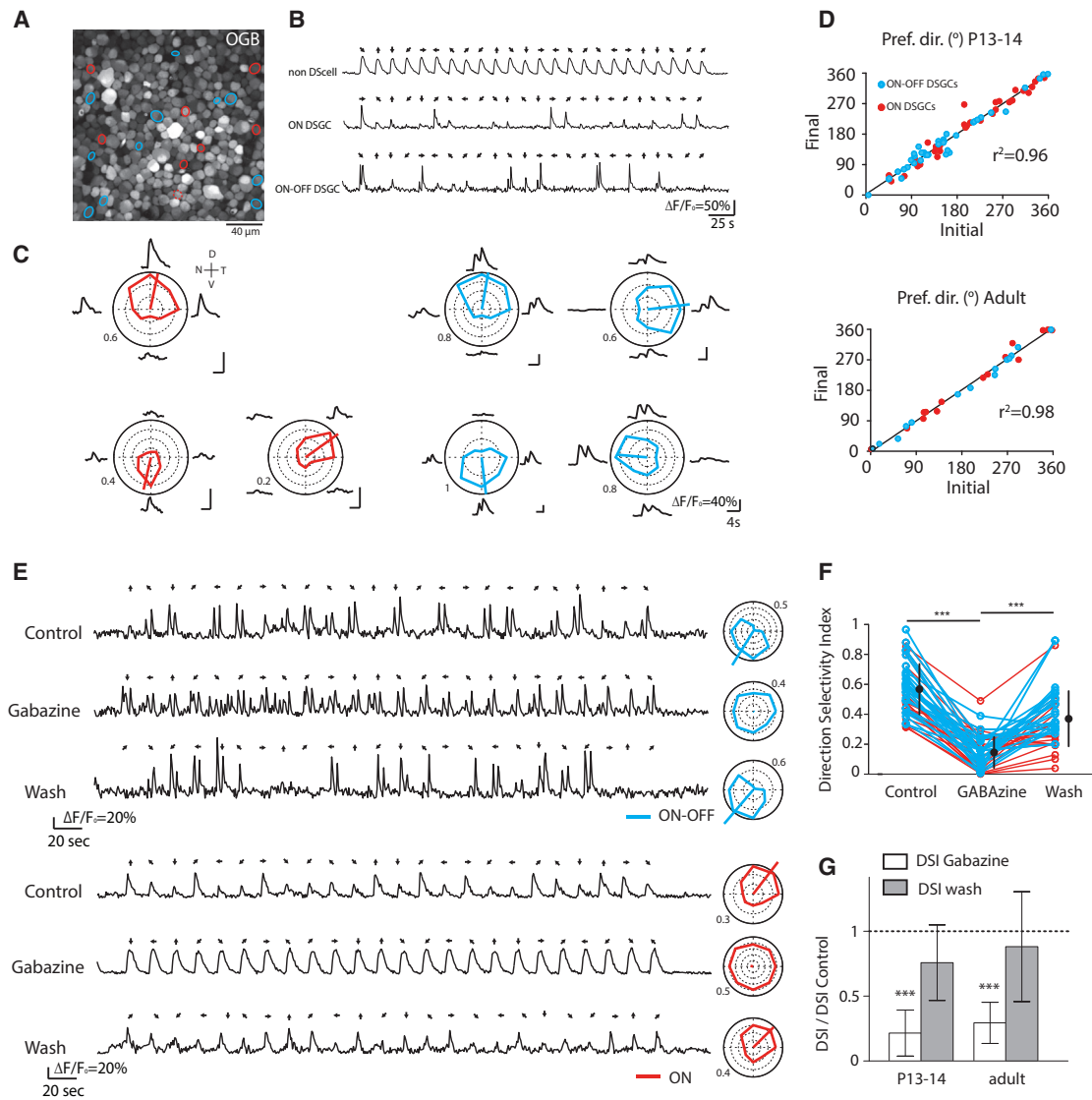


**Figure 1. Two-Photon Calcium Imaging Reliably Identifies Both ON and ON-OFF DSGCs in Response to UV-Drifting Bars**

(A) Two-photon fluorescent image of OGB-1 in ganglion cell layer of P13 retina. Red and blue circles indicate ON and ON-OFF DSGCs, respectively.

(B) Examples of OGB-1 calcium signals ( $\Delta F/F_0$ ) in response to a UV bar moving in eight different directions (black arrows).

(C) Average calcium responses ( $\Delta F/F_0$ ) and tuning curves of three ON DSGCs and four ON-OFF DSGCs from the same field of view in response to a UV-drifting bar. The colored lines inside the polar plots indicate the vector sum. Numbers around polar plots are indicating the amplitude of calcium signals ( $\Delta F/F_0$ ). V, ventral; N, nasal; D, dorsal; T, temporal.

(D) Preferred directions remain stable between two consecutive imaging sessions for both ON (red) and ON-OFF DSGCs (blue) at eye-opening (top,  $n = 73$  cells from three retinas) and in adult (bottom,  $n = 30$  cells from two retinas). Pref. dir., preferred direction.  $r^2$  indicates the measure of goodness of fit of linear regression.

(E) Examples of OGB-1 calcium signals ( $\Delta F/F_0$ ) from an ON-OFF DSGC (top) and an ON DSGC (bottom) in the same field of view from a P14 retina before (top),

after 15-min bath application of GABA<sub>A</sub> receptor blocker (GABAzine, 10  $\mu$ M; middle) and after 30 min of rinsing (bottom). Tuning curves for each condition are shown on right.

(F) Direction-selective index of ON DSGCs (red) and ON-OFF DSGCs (blue) from P13–P14 and adult retinas before, during, and after GABAzine application. Black circles and error bars show mean  $\pm$  SD (\*\*\* $p < 0.001$ , one-way ANOVA with Tukey post hoc test).

(G) Summary effects of GABAzine (5–10  $\mu$ M; white bars) and its rinse (gray bars) on the direction-selective index (DSI) as compared to control at eye-opening (left,  $n = 36$  DSGCs with 16 ON DSGCs and 20 ON-OFF DSGCs from two retinas) and in adult (right,  $n = 20$  DSGCs with 12 ON DSGCs and 8 ON-OFF DSGCs from two retinas). Means and SD are shown. (\*\*\* $p < 0.001$ , one-way ANOVA with Tukey post hoc test.)

See also [Figure S1](#) and [Table S1](#).

ON-OFF DSGCs were more broadly distributed than in adult ([Figure 2A](#)), similar to rabbit [20]. We note that this lack of clustering along the cardinal axes was observed in individual retinas

([Figure S2](#)) and therefore was not due to variations in retinal positioning in the recording chamber. Interestingly, ON-DSGCs mostly avoided nasal preferred directions, indicating a strong

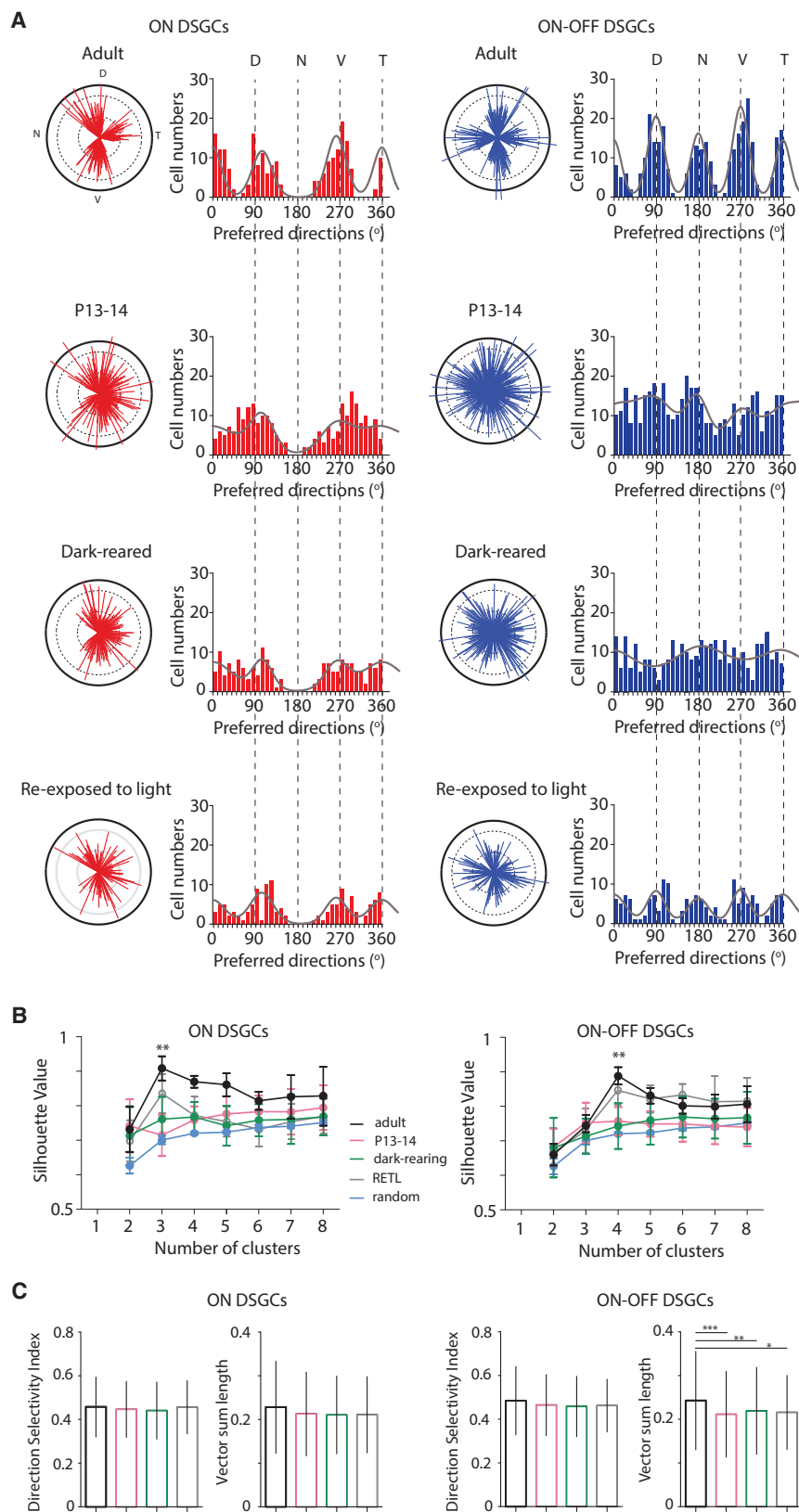


**Figure 2. Clustering of the Preferred Directions of ON and ON-OFF DSGCs along the Cardinal Axes Requires Visual Experience**

(A) The preferred directions are plotted as polar plots (left) and histograms (right) for ON DSGCs (red) and ON-OFF DSGCs (blue) in adult (top), at eye-opening (middle top), after dark-rearing (middle bottom) and after re-exposure the dark-reared mice to a normal light cycle (12 hr darkness: 12 hr light) for 30–50 days (bottom). Solid black lines of polar plots indicate a vector sum length of 0.5 (see the [Supplemental Information](#) for definition). Solid gray lines on the histograms indicate the von Mises distributions with fixed angles ( $0^\circ$ ,  $105^\circ$ , and  $263^\circ$  for ON DSGCs and  $0^\circ$ ,  $90^\circ$ ,  $180^\circ$ , and  $270^\circ$  for ON-OFF DSGCs).

(B) Average silhouette values as a function of the different cluster numbers for ON DSGCs (left) and ON-OFF DSGCs (right) in adult (black line), at P13–P14 (magenta), after dark-rearing (green), after re-exposure to light (gray) and in random distribution (blue). Silhouette values were calculated using k-means clustering analysis of the preferred directions observed in (A). Mean and SD are given for each cluster (\*\* $p < 0.01$ , one-way ANOVA with Tukey post hoc test).

(C) Direction selectivity index and tuning strength represented by the vector sum length of ON (left) and ONOFF (right) DSGCs in adult (black), P13–P14 (magenta), dark-reared (green), and dark-reared mice re-exposed to light (gray).

Mean and SD are represented (\* $p < 0.05$ , \*\* $p < 0.01$ , \*\*\* $p < 0.001$  one-way ANOVA with Tukey post hoc test). See also [Figures S2](#) and [S3](#) and [Tables S2](#) and [S3](#).

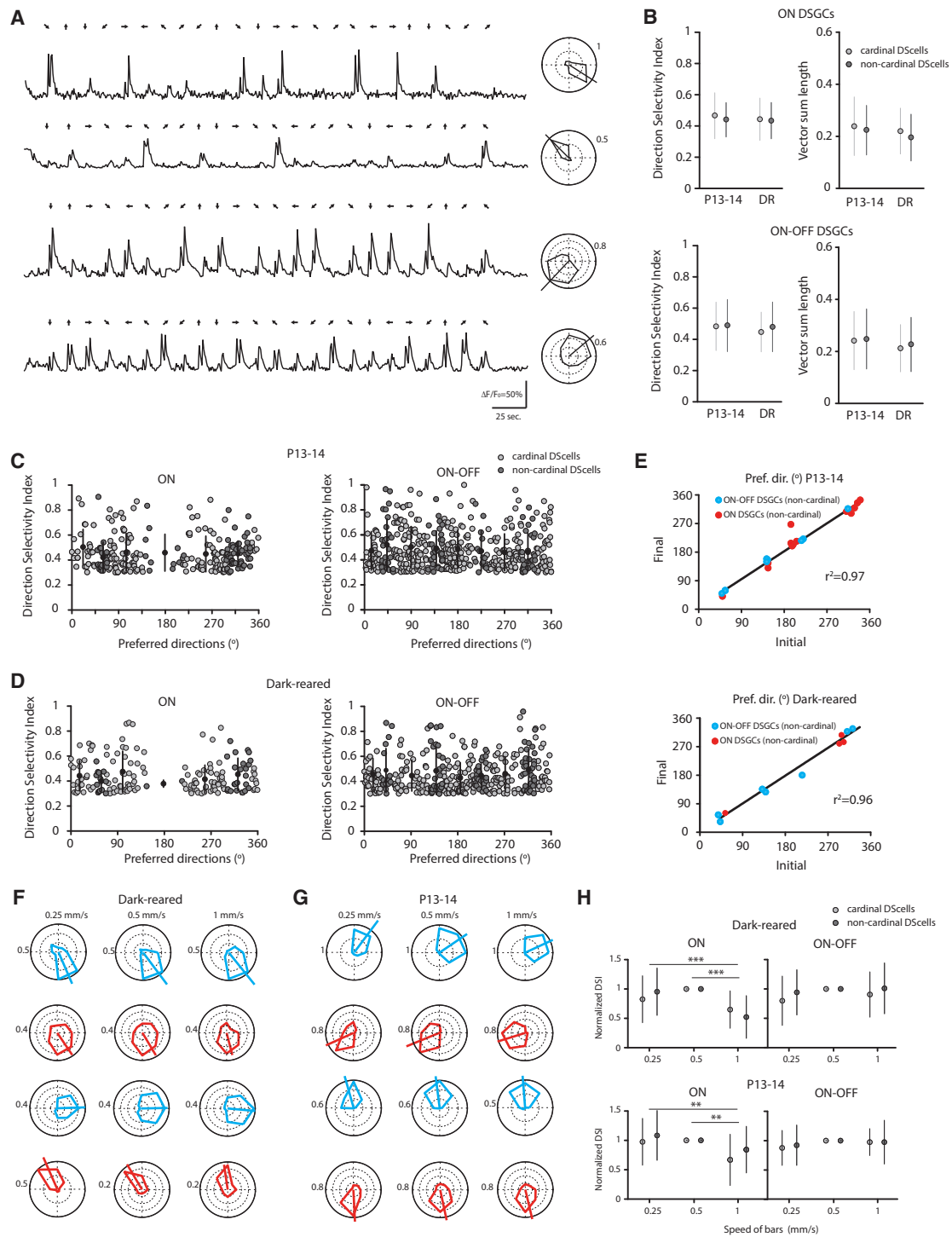


**Figure 3. Non-cardinal DSGCs Do Not Display Broader Direction-Selective Tuning or Distinct Speed-Tuning**

(A) Examples of OGB-1 calcium signals ( $\Delta F/F_0$ ) from four non-cardinal ON-OFF DSGCs in a P13 retina with tuning curves shown at right. Numbers around polar plots are indicating the amplitude of calcium signals ( $\Delta F/F_0$ ).

(B) Direction selectivity index and magnitude of the vector sum of ON DSGCs (top) and ON-OFF DSGCs (bottom) that are aligned (light gray circles, cardinal) or not aligned (dark gray circles, non-cardinal) along the cardinal axes at eye-opening (P13–P14,  $n = 157$  cardinal ON DSGCs and  $n = 88$  non-cardinal ON DSGCs;  $n = 330$  cardinal ON-OFF DSGCs and  $n = 103$  non-cardinal ON-OFF DSGCs from seven retinas) and after dark-rearing (DR,  $n = 132$  cardinal ON DSGCs and  $n = 39$  non-cardinal ON DSGCs;  $n = 229$  cardinal ON-OFF DSGCs and  $n = 108$  non-cardinal ON-OFF DSGCs from six retinas). ( $p > 0.05$ , one-way ANOVA with Tukey post hoc test.) Mean and SD are shown.

(legend continued on next page)

repulsive signal for that direction. Our findings indicate that the preferred directions for ON and ON-OFF DSGCs cluster along the cardinal axes within three weeks after eye-opening.

To test whether this clustering is dependent on visual experience, we measured the tuning properties in WT mice that were dark-reared from P3 to adult (>P30). Surprisingly, we found that dark-rearing prevented the clustering of the preferred directions of both ON and ON-OFF DSGC along the cardinal axes (Figure 2A; Figure S2). Re-exposure to light for 30–50 days following dark rearing leads to clustering of ON-OFF and ON DSGCs along the cardinal axes (Figures 2 and S2; Table S2), though many cells retained preferred directions along non-cardinal axes. This partial rescue of the phenotype indicates that there is not a strict critical period for the development of retinal direction selectivity.

To compare quantitatively the distributions of preferred directions for P13–P14, adult light-reared, adult dark-reared, and dark-reared mice that were re-exposed to light, we used three methods. First, we fit each DSGC population's distribution of preferred directions to a mixture model composed of three von Mises (VM) distributions for ON cells and four VM distributions for ON-OFF cells, using maximum likelihood estimation (Figure 2A; Table S2). Adult DSGC populations for both ON and ON-OFF cells were well fit with narrower VM distributions, while P13–P14 and dark-reared populations were fit by broader VM distributions, indicating that adult DSGCs display stronger clustering than their P14 and dark-reared counterparts. This effect was more pronounced for the vertically tuned ON-OFF DSGCs (Table S2). Again, the fits indicate that the clustering was partially recovered upon re-exposure to light.

Second, we used circular statistics to compare distributions of preferred directions and determined significant differences between adult, P13–P14 and dark-reared ON and ON-OFF DSGCs (Figure S3; Table S3). We found that in dark-reared mice re-exposed to light, ON-OFF DSGCs, but not ON-DSGCs, were also significantly different than light-reared adults.

Third, we used a k-means clustering algorithm [21] to determine the number of clusters that best describes the distribution pattern of the preferred directions of DSGCs (Figure 2B). To compare the extent of clustering, we computed the silhouette value, with higher silhouette values indicating an appropriate number of clusters [20, 21] (see the Supplemental Information). Adult retinas displayed significantly higher silhouette values for three and four specific clusters for the ON and the ON-OFF DSGCs, respectively, than a random distribution of preferred directions (0.91 and 0.89). In contrast, neither young nor dark-reared retinas showed a peak in their silhouette values for any cluster number. Thus, at eye-opening and in dark-reared adult

retina, both ON and ON-OFF DSGCs display distributions of preferred directions that are not significantly different from a random distribution of preferred directions. Consistent with previous measures (Figure 2), re-exposure to light partially reverses this effect. Significantly higher silhouette values were observed for three and four specific clusters for the ON and the ON-OFF DSGCs, respectively, compared to a random distribution of preferred directions (0.87 and 0.85) (Figure 2B).

To determine the effect of dark rearing on DS tuning, we compared two measures of tuning—direction-selective index (DSI) and the magnitude of the vector sum—for the different conditions (Figure 2C). We found no significant difference for the DSIs of either ON and ON-OFF DSGCs across conditions [3, 6], and a small but significant increase in the vector sum for ON-OFF DSGCs across development, as described previously [5, 8], suggesting a visually driven maturation of tuning properties. Though DSGCs were strongly tuned at eye-opening and after dark-rearing, both ON and ON-OFF DSGCs in young and dark-reared mice retained the immature distribution of preferred directions, failing to cluster along the cardinal axes (Figure 2; Figure S2).

Finally, we found that dark-rearing led to a higher percentage of non-responsive cells (Table S1), as well as and a small but significant decrease (~5%) in calcium transient amplitudes of ON responses, but not OFF responses, from DSGCs. This is consistent with previous studies demonstrating that visual deprivation weakens excitatory input into RGCs [22] and alters the synaptic connectivity between cones and ON bipolar cells [23] or between bipolar cells and their postsynaptic targets.

Together, these results indicate that the primary impact of visual experience is on clustering of ON and ON-OFF DSGCs preferred directions along their cardinal directions rather than on the development of their light response or directional tuning.

### Clustering along Cardinal Axes Occurs via Realignment Rather Than Refinement of Directional Tuning

How does visual experience induce the clustering of preferred directions? As a first step toward answering this question, we investigated whether clustering occurs via refinement, i.e., a sharpening or stabilizing of DSGC directional tuning. We compared the strength of directional tuning for DSGCs aligned along the cardinal axes to that of DSGCs not aligned along these axes, which we term non-cardinal DSGCs (see the Supplemental Information). We found that non-cardinal DSGCs exhibited similar calcium transient amplitudes and directional tuning properties (DSI and magnitude of the vector sum) to cardinal-axes

(C and D) Direction-selectivity index as a function of the preferred directions of ON DSGCs (left) and ON-OFF DSGCs (right) that are aligned (light-gray circles) or not aligned (dark-gray circles) along the cardinal axes at P13–P14 ( $n = 245$  ON DSGCs and  $n = 433$  ON-OFF DSGCs from seven retinas) and after dark-rearing ( $n = 171$  ON DSGCs and  $n = 337$  ON-OFF DSGCs from six retinas). Each circle represents one DSGC. Mean and SD are shown.

(E) Preferred directions are stable between two consecutive imaging sessions for non-cardinal ON (red) and ON-OFF DSGCs (blue) at eye-opening (top,  $n = 23$  cells from three retinas) and after dark-rearing (bottom,  $n = 12$  cells from two retinas). Pref. dir., preferred direction.

(F and G) Speed tuning of non-cardinal (top) and cardinal (bottom) ON-OFF (blue) and ON (red) DSGCs as assessed by three different bar speeds (left, 0.25 mm/s; middle, 0.5 mm/s; right, 1 mm/s) from adult dark-reared (F) and P13–P14 (G) retinas.

(H) Comparison of the speed tuning from cardinal (light-gray circles) and non-cardinal (dark-gray circles) ON (left) and ON-OFF (right) DSGCs. DSIs were normalized to the value recorded at 0.5 mm/s in dark-reared (top,  $n = 37$  cardinal ON DSGCs and  $n = 30$  non-cardinal ON DSGCs;  $n = 69$  cardinal ON-OFF DSGCs and  $n = 31$  non-cardinal ON-OFF DSGCs) and young mice (bottom,  $n = 19$  cardinal ON DSGCs and  $n = 12$  non-cardinal ON DSGCs;  $n = 65$  cardinal ON-OFF DSGCs and  $n = 17$  non-cardinal ON-OFF DSGCs) (\*\* $p < 0.01$ , \*\*\* $p < 0.001$ , one-way ANOVA with Tukey post hoc test). Mean and SD are shown.

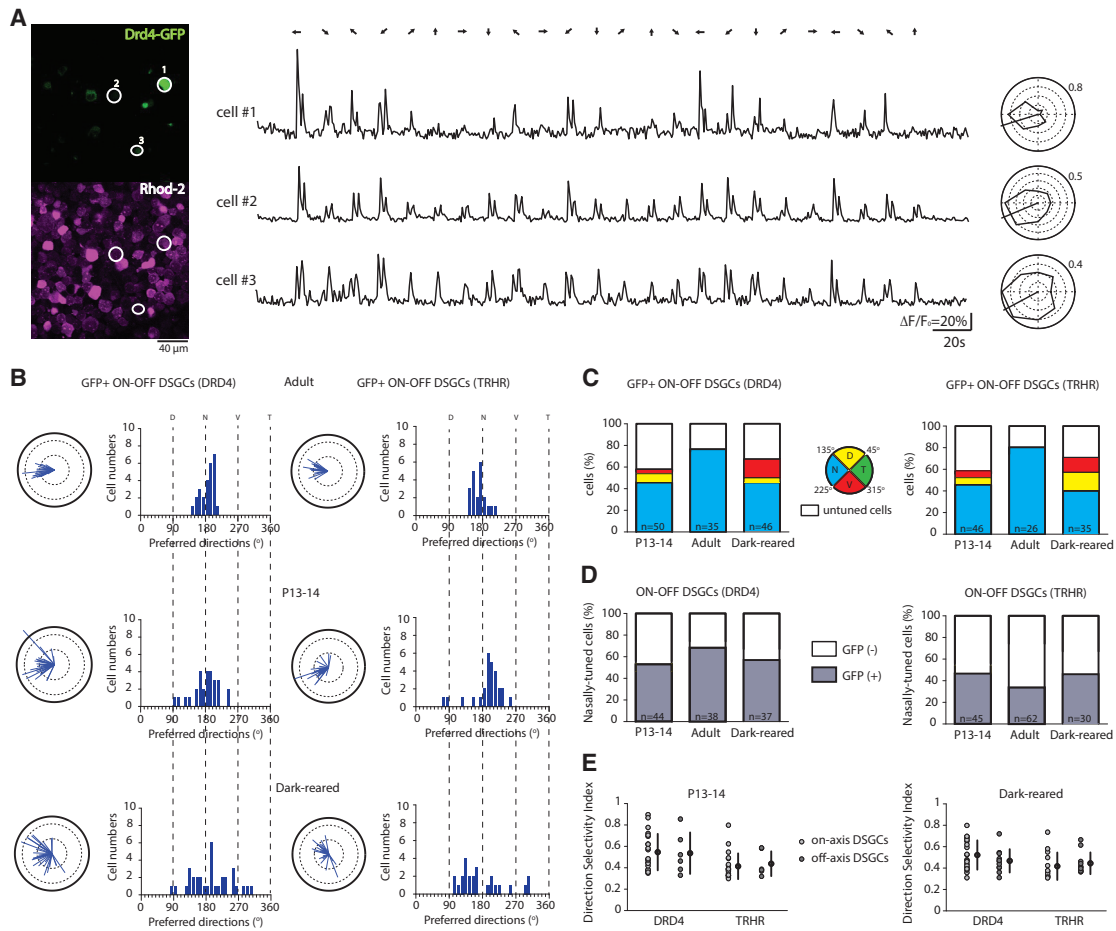


**Figure 4. Clustering of GFP<sup>+</sup> DSGCs along the Cardinal Axes Occurs by a Process of Realignment that Depends on Visual Experience**

(A) Two-photon fluorescent images (left) show the GFP signal (top, green channel) and the calcium dye Rhod-2 signal (bottom, red channel) in the ganglion cell layer of a P14 *Drd4*-GFP mouse. The three white-circled GFP<sup>+</sup> ON-OFF DSGCs produce the shown Rhod-2 calcium responses ( $\Delta F/F_0$ ) (middle) and tuning curves (right). All have the same nasally oriented direction. Numbers around polar plots are indicating the amplitude of calcium signals ( $\Delta F/F_0$ ).

(B) Polar plots and histograms of preferred directions for GFP<sup>+</sup> ON-OFF DSGCs from DRD4-GFP mice (left) and TRHR-GFP mice (right) in adult (top), at eye-opening (middle) and after dark-rearing (bottom). Solid black lines of polar plots indicate a vector sum length of 0.5 (see the Supplemental Information for definition).

(C) Percentage of GFP<sup>+</sup> ON-OFF DSGCs (DRD4-GFP line, left; TRHR-GFP line, right) that are nasally (N, blue), dorsally (D, yellow), ventrally (V, red) tuned or untuned (white) at eye-opening (P13–P14), in adult and after dark-rearing. Total number of imaged GFP<sup>+</sup> cells is given within bars.

(D) Percentage of nasally tuned ON-OFF DSGCs (DRD4-GFP line, left; TRHR-GFP line, right) that are GFP<sup>+</sup> (gray) or GFP<sup>-</sup> (white) at eye-opening (P13–P14), in adult and after dark-rearing. Total number of imaged nasally tuned DSGCs is indicated within bars.

(E) Direction selectivity index of cardinal (light gray circle) and non-cardinal (dark-gray circle) ON-OFF DSGCs from DRD4-GFP and TRHR-GFP mice at P13–P14 (left) and after dark-rearing (right) ( $p > 0.05$ , Mann-Whitney t test). Means and SD are shown.

See also Figure S4 and Table S4.

DSGCs (Figures 3A–3D). Moreover, in young and dark-reared retinas the preferred directions of non-cardinal ON and ON-OFF DSGCs remained stable in two consecutive imaging sessions (Figure 3E). Thus, non-cardinal tuning is not the result of broader directional tuning that would cause the preferred direction to be more variable [24]. Furthermore, non-cardinal DSGCs exhibited the same velocity tuning as cardinal DSGCs in both in young and dark-reared mice (Figures 3F and 3G). Together, these results suggest that visually driven clustering is not due to the relative timing of the excitatory and inhibitory inputs onto DSGCs [25].

We next investigated whether vision causes non-cardinal DSGCs to realign their tuning to a cardinal direction. We

repeated our experiments in two transgenic mouse lines—*Drd4*-GFP [26] and *Trhr*-GFP [27]—that express GFP in the DSGC subtype that prefers motion only along the nasal direction. To enable simultaneous imaging of GFP and calcium transients, we used a red-calcium dye, Rhod-2 [9, 28] (Figure 4A). We first confirmed in adult retina that the majority of GFP<sup>+</sup> cells were ON-OFF DSGCs (~74% for *Drd4* and ~81% for *Trhr*), a fraction consistent with a previous report based on targeted recordings [27]. We found that the vast majority of these DSGCs preferred directions clustering along the nasal axis (Table S4). Of note, in *Trhr*-GFP and *Drd4*-GFP mice, the GFP<sup>+</sup> cells constituted 34% (21/62) and 68% (26/38), respectively, of all nasally tuned DSGCs in adult, indicating that neither line fully represents this



subtype of ON-OFF DSGCs. To ensure that we were not undercounting due to dim GFP fluorescence, we compared the cell densities based on retinas immuno-stained for GFP either before or after the electroporation of Rhod-2. We did not observe any significant differences between these three conditions for *Drd4* and *Trhr* lines in P13–P14, adult or dark-reared retinas (Table S4).

Similar to our results for all DSGCs, these genetically identifiable subtypes of DSGC exhibited a broader distribution of preferred directions at eye-opening and after dark-rearing than in adult (Figures 4B and 4C). Compared to adult retinas, we observed a larger percentage of non-cardinal (i.e., non-nasally tuned) GFP<sup>+</sup> neurons at P14 (*Drd4*, 12% ± 4%; *Trhr*, 13% ± 3%; Figure 4C; Table S4) and after dark-rearing (*Drd4*, 21% ± 5%; *Trhr*, 31% ± 8%, Figure 2C; Table S4). Note, the strength of directional tuning for non-cardinal GFP<sup>+</sup> DSGCs did not differ significantly from cardinal GFP<sup>+</sup> DSGCs in either transgenic lines (*Drd4* and *Trhr*) (Figure 4E), indicating that the non-cardinal axes tuning is not caused by weaker tuning properties. In addition, we did not observe higher cell densities of the ON and the ON-OFF DSGCs in young or dark-reared retinas compared to adult (Table S1) ruling out the possibility that non-cardinal DSGCs lose their direction selectivity rather than realigning along the cardinal axes.

Last, we tested whether dark-rearing altered the morphology of DSGCs. In mice, dark-rearing changes the dendritic stratification [15, 29] and dendritic branching patterns [30] of non-direction-selective RGCs. However, in rabbits, dark-reared DSGCs display dendritic features that are similar to normally reared DSGCs [3]. GFP<sup>+</sup> DSGCs in both *Trhr* and *Drd4* mice were filled with a fluorescent dye via a whole-cell pipette and subsequently imaged. We found that dark-rearing did not alter the morphology of DSGC dendritic arborizations (Figure S4).

Together, these experiments indicate that visual experience clusters the preferred directions of DSGCs not by narrowing the directional tuning but via visual experience-dependent realignment.

## DISCUSSION

We find that although ON and ON-OFF DSGCs are detectable at eye-opening in mice, their preferred directions are not clustered along the cardinal axes as in adult. Moreover, this clustering does not emerge in dark-reared animals. Our findings indicate, for the first time, that visual experience plays a critical role in the development of one aspect of directional selectivity within the mouse retina, namely, the clustering of preferred directions along the cardinal axes. Thus, visual experience plays a crucial role in shaping receptive field properties in the retina.

### Distribution of DSGC Preferred Directions along the Cardinal Axes Changes over Development

In contrast to our results reported here, previous reports from our laboratory that were based on multi-electrode array (MEA) recordings indicated that the cardinal distribution of preferred directions was established at eye-opening [5]. One potentially important difference is that the current study is based on light stimulation of cones dominated by S opsin in ventral retina [13, 14] to evoke DSGC responses while our previous study used visible light to stimulate cones dominated by M opsin in dorsal retina. Since mouse retina exhibits delayed expression of M

opsin immunoreactive cones compared to S cones [31], MEA may have recorded fewer numbers of DSGCs at eye-opening. In fact, quantification of clustering by applying the k-clustering analysis to our previous MEA data does in fact indicate a lack of clustering at P14 [20]. Hence, our findings here agree with previous studies and with more recent single-cell extracellular recordings from rabbit retina that also indicate a lack of clustering at eye-opening [20].

A second difference with the previous MEA study is that alignment of the preferred directions along the temporal and ventral quadrants are overrepresented [5, 32], a bias that persists in recordings from V1 at eye-opening [33] but was not seen here (Figure 2; Figure S3). Interestingly, it was recently shown that DSGC preferred directions vary retinotopically (S. Sabbah et al., 2015, Association for Research in Vision and Ophthalmology, abstract); hence, recordings in dorsal retina may show a different distribution of preferred directions than recordings in ventral retina. Additional work is necessary to determine whether this retinotopy of preferred directions is observed for both ON and ON-OFF DSGC subtypes.

### Potential Activity-Dependent Mechanisms

How could visual experience alter the distribution of DSGC preferred directions? The predominant model for direction selectivity is that the null axis is determined by the precise wiring of GABAergic starburst amacrine cells (SACs) onto the different subtypes of ON and ON-OFF DSGCs [1]. Hence, refinement of inhibitory connectivity from null-oriented SAC processes to DSGCs may contribute to the clustering of preferred directions along the cardinal axes. Prior to eye-opening, there is an increase in the number of functional inhibitory synapses from the null-oriented SAC processes to DSGCs [7, 16, 17]. In adult, serial EM reconstructions indicate that a given SAC branch, which is activated most strongly by centrifugal motion, preferentially, but not exclusively, synapses onto one DSGC subtype [34]. Therefore, one possibility is that after dark-rearing, the wiring of SACs to DSGCs is less precise in that a given SAC branch is not as particular and forms many synapses with different DSGCs, and thus a given DSGC receives inputs from SAC branches of different orientations. Note in this scenario the tuning width of DSGCs could remain narrow despite the integration of different orientations if tuning were determined by postsynaptic non-linearities, such as dendritic spiking [35].

A second possibility is that visual experience facilitates the maturation of SAC-SAC connectivity. For example, deleting protocadherins in SACs leads to a loss of self-avoidance between SACs [36] and produces a broader distribution of preferred directions for ventrally tuned DSGCs. Indeed, the connections between closely spaced SACs do undergo an age-dependent decrease. Hence, vision-dependent refinement of SAC-SAC connectivity may play a role in clustering DSGC preferred directions along the cardinal axes.

A third possibility is that visual experience acts to reduce gap junction coupling among DSGCs of different preferred directions. Near eye-opening, there is robust gap junction coupling among different DSGC subtypes [37], while in adult only the superior-preferring DSGC subtype is coupled [38–40]. Hence, each DSGC may be tuned to a cardinal axis, but input via a gap junction from a DSGC tuned to a different cardinal direction may

cause the final tuning of the DSGC to lie off its cardinal axis. Previous studies indicate that dark-rearing delayed the decoupling process but did not prevent it. Hence, this decoupling is not likely to mediate this effect.

Regardless of the mechanisms that underlie the influence of visual experience, there is a more fundamental question, does visual experience play an instructive or permissive role in the alignment of DSGC preferred directions along cardinal axes? An instructive role is supported by the argument that there is more power in natural scenes along cardinal axes [41, 42] in the sense that the ability to perceive contours that are vertically or horizontally oriented is greater than the ability to perceive oblique angles. However, whether this is the case for mice still remains to be determined [43].

We found that visual deprivation led to a broader distribution of the DSGCs preferred directions than what is found early in development (Figures 2 and S2; Table S2), indicating that dark-rearing may be not only preventing visually guided maturation, but also inducing pathological effects on the retina. However, previous studies indicate that dark-rearing has either a transient impact on RGC properties (reviewed in [44]) or a small effect on spatio-temporal properties of RGCs, many other response properties are maintained [45]. Indeed, we find that in dark-reared mice, directional and speed tuning are maintained, indicating limited impact of overall circuit function. Dark-rearing has been implicated in a delay in the maturation of cone-cone bipolar cell synapses [23], which may explain the slightly reduced number of light-responsive cells we observed (Table S1). It has also been implicated in changes in RGC stratification [44]. However, we observed no difference in morphology of DSGCs, in that reconstructed GFP<sup>+</sup> DSGCs in adult dark-reared mice (Figure S4) maintain normal bi-stratification of dendritic arbors and a significant dendritic overlap between neighboring homotypic subtypes as is seen in normal-reared mice [27]. Finally, we found that re-exposure to light partially reverses the clustering of DSGCs along the cardinal axes (Figure 2; Table S2) contrary to the existence of a critical period described in V1 ferrets [46].

#### SUPPLEMENTAL INFORMATION

Supplemental Information includes Supplemental Experimental Procedures, four figures, and four tables and can be found with this article online at <http://dx.doi.org/10.1016/j.cub.2016.03.073>.

#### AUTHOR CONTRIBUTIONS

R.B. and M.B.F. designed the experiments. R.B. performed all the experiments. R.B. and C.G. performed the analysis of the two-photon calcium imaging experiments and the statistical tests. R.B. and M.B.F. wrote the manuscript.

#### ACKNOWLEDGMENTS

We are grateful to David Arroyo, Ryan Morrie, and Rick Ayer (Sutter Instruments, Novato, CA) for technical support and members of M.B.F.'s lab for discussion. R.B. and M.B.F. were supported by NIH RO1EY019498, RO1EY013528, and C.G. was supported by P30EY003176.

Received: January 10, 2016

Revised: March 8, 2016

Accepted: March 31, 2016

Published: May 5, 2016

#### REFERENCES

1. Vaney, D.I., Sivyer, B., and Taylor, W.R. (2012). Direction selectivity in the retina: symmetry and asymmetry in structure and function. *Nat. Rev. Neurosci.* *13*, 194–208.
2. Yonehara, K., Ishikane, H., Sakuta, H., Shintani, T., Nakamura-Yonehara, K., Kamiji, N.L., Usui, S., and Noda, M. (2009). Identification of retinal ganglion cells and their projections involved in central transmission of information about upward and downward image motion. *PLoS ONE* *4*, e4320.
3. Chan, Y.-C., and Chiao, C.-C. (2008). Effect of visual experience on the maturation of ON-OFF direction selective ganglion cells in the rabbit retina. *Vision Res.* *48*, 2466–2475.
4. Sun, L., Han, X., and He, S. (2011). Direction-selective circuitry in rat retina develops independently of GABAergic, cholinergic and action potential activity. *PLoS ONE* *6*, e19477.
5. Elstrott, J., Anishchenko, A., Greschner, M., Sher, A., Litke, A.M., Chichilnisky, E.J., and Feller, M.B. (2008). Direction selectivity in the retina is established independent of visual experience and cholinergic retinal waves. *Neuron* *58*, 499–506.
6. Chen, M., Weng, S., Deng, Q., Xu, Z., and He, S. (2009). Physiological properties of direction-selective ganglion cells in early postnatal and adult mouse retina. *J. Physiol.* *587*, 819–828.
7. Wei, W., Hamby, A.M., Zhou, K., and Feller, M.B. (2011). Development of asymmetric inhibition underlying direction selectivity in the retina. *Nature* *469*, 402–406.
8. Chen, H., Liu, X., and Tian, N. (2014). Subtype-dependent postnatal development of direction- and orientation-selective retinal ganglion cells in mice. *J. Neurophysiol.* *112*, 2092–2101.
9. Briggman, K.L., and Euler, T. (2011). Bulk electroporation and population calcium imaging in the adult mammalian retina. *J. Neurophysiol.* *105*, 2601–2609.
10. Vlasits, A.L., Bos, R., Morrie, R.D., Fortuny, C., Flannery, J.G., Feller, M.B., and Rivlin-Etzion, M. (2014). Visual stimulation switches the polarity of excitatory input to starburst amacrine cells. *Neuron* *83*, 1172–1184.
11. Gauvain, G., and Murphy, G.J. (2015). Projection-specific characteristics of retinal input to the brain. *J. Neurosci.* *35*, 6575–6583.
12. Baden, T., Berens, P., Franke, K., Román Rosón, M., Bethge, M., and Euler, T. (2016). The functional diversity of retinal ganglion cells in the mouse. *Nature* *529*, 345–350.
13. Wang, Y.V., Weick, M., and Demb, J.B. (2011). Spectral and temporal sensitivity of cone-mediated responses in mouse retinal ganglion cells. *J. Neurosci.* *31*, 7670–7681.
14. Baden, T., Schubert, T., Chang, L., Wei, T., Zaichuk, M., Wissinger, B., and Euler, T. (2013). A tale of two retinal domains: near-optimal sampling of achromatic contrasts in natural scenes through asymmetric photoreceptor distribution. *Neuron* *80*, 1206–1217.
15. Tian, N., and Copenhagen, D.R. (2003). Visual stimulation is required for refinement of ON and OFF pathways in postnatal retina. *Neuron* *39*, 85–96.
16. Yonehara, K., Balint, K., Noda, M., Nagel, G., Bamberg, E., and Roska, B. (2011). Spatially asymmetric reorganization of inhibition establishes a motion-sensitive circuit. *Nature* *469*, 407–410.
17. Morrie, R.D., and Feller, M.B. (2015). An asymmetric increase in inhibitory synapse number underlies the development of a direction selective circuit in the retina. *J. Neurosci.* *35*, 9281–9286.
18. Dhande, O.S., Estevez, M.E., Quattrochi, L.E., El-Danaf, R.N., Nguyen, P.L., Berson, D.M., and Huberman, A.D. (2013). Genetic dissection of retinal inputs to brainstem nuclei controlling image stabilization. *J. Neurosci.* *33*, 17797–17813.
19. Fiscella, M., Franke, F., Farrow, K., Müller, J., Roska, B., da Silveira, R.A., and Hierlemann, A. (2015). Visual coding with a population of direction-selective neurons. *J. Neurophysiol.* *114*, 2485–2499.

20. Chan, Y.-C., and Chiao, C.-C. (2013). The distribution of the preferred directions of the ON-OFF direction selective ganglion cells in the rabbit retina requires refinement after eye opening. *Physiol. Rep.* *1*, e00013.
21. Rousseeuw, P.J. (1987). Silhouettes - a graphical aid to the interpretation and validation of cluster-analysis. *J. Comput. Appl. Math.* *20*, 53–65.
22. Tian, N., and Copenhagen, D.R. (2001). Visual deprivation alters development of synaptic function in inner retina after eye opening. *Neuron* *32*, 439–449.
23. Dunn, F.A., Della Santina, L., Parker, E.D., and Wong, R.O. (2013). Sensory experience shapes the development of the visual system's first synapse. *Neuron* *80*, 1159–1166.
24. Stryker, M.P., Sherk, H., Leventhal, A.G., and Hirsch, H.V. (1978). Physiological consequences for the cat's visual cortex of effectively restricting early visual experience with oriented contours. *J. Neurophysiol.* *41*, 896–909.
25. Sivyer, B., van Wyk, M., Vaney, D.I., and Taylor, W.R. (2010). Synaptic inputs and timing underlying the velocity tuning of direction-selective ganglion cells in rabbit retina. *J. Physiol.* *588*, 3243–3253.
26. Huberman, A.D., Wei, W., Elstrott, J., Stafford, B.K., Feller, M.B., and Barres, B.A. (2009). Genetic identification of an On-Off direction-selective retinal ganglion cell subtype reveals a layer-specific subcortical map of posterior motion. *Neuron* *62*, 327–334.
27. Rivlin-Etzion, M., Zhou, K., Wei, W., Elstrott, J., Nguyen, P.L., Barres, B.A., Huberman, A.D., and Feller, M.B. (2011). Transgenic mice reveal unexpected diversity of on-off direction-selective retinal ganglion cell subtypes and brain structures involved in motion processing. *J. Neurosci.* *31*, 8760–8769.
28. Minta, A., Kao, J.P., and Tsien, R.Y. (1989). Fluorescent indicators for cytosolic calcium based on rhodamine and fluorescein chromophores. *J. Biol. Chem.* *264*, 8171–8178.
29. Xu, H.-P., and Tian, N. (2007). Retinal ganglion cell dendrites undergo a visual activity-dependent redistribution after eye opening. *J. Comp. Neurol.* *503*, 244–259.
30. Xu, H.-P., Sun, J.H., and Tian, N. (2014). A general principle governs vision-dependent dendritic patterning of retinal ganglion cells. *J. Comp. Neurol.* *522*, 3403–3422.
31. Szél, A., Röhlich, P., Mieziwska, K., Aguirre, G., and van Veen, T. (1993). Spatial and temporal differences between the expression of short- and middle-wave sensitive cone pigments in the mouse retina: a developmental study. *J. Comp. Neurol.* *331*, 564–577.
32. Yonehara, K., Fiscella, M., Drinnenberg, A., Esposti, F., Trenholm, S., Krol, J., Franke, F., Scherf, B.G., Kusnyerik, A., Müller, J., et al. (2016). Congenital Nystagmus Gene FRMD7 Is Necessary for Establishing a Neuronal Circuit Asymmetry for Direction Selectivity. *Neuron* *89*, 177–193.
33. Rochefort, N.L., Narushima, M., Grienberger, C., Marandi, N., Hill, D.N., and Konnerth, A. (2011). Development of direction selectivity in mouse cortical neurons. *Neuron* *71*, 425–432.
34. Briggman, K.L., Helmstaedter, M., and Denk, W. (2011). Wiring specificity in the direction-selectivity circuit of the retina. *Nature* *471*, 183–188.
35. Sivyer, B., and Williams, S.R. (2013). Direction selectivity is computed by active dendritic integration in retinal ganglion cells. *Nat. Neurosci.* *16*, 1848–1856.
36. Kostadinov, D., and Sanes, J.R. (2015). Protocadherin-dependent dendritic self-avoidance regulates neural connectivity and circuit function. *eLife* *4*, 4.
37. Xu, Z., Zeng, Q., Shi, X., and He, S. (2013). Changing coupling pattern of The ON-OFF direction-selective ganglion cells in early postnatal mouse retina. *Neuroscience* *250*, 798–808.
38. Trenholm, S., McLaughlin, A.J., Schwab, D.J., and Awatramani, G.B. (2013). Dynamic tuning of electrical and chemical synaptic transmission in a network of motion coding retinal neurons. *J. Neurosci.* *33*, 14927–14938.
39. DeBoer, D.J., and Vaney, D.I. (2005). Gap-junction communication between subtypes of direction-selective ganglion cells in the developing retina. *J. Comp. Neurol.* *482*, 85–93.
40. Weng, S., Sun, W., and He, S. (2005). Identification of ON-OFF direction-selective ganglion cells in the mouse retina. *J. Physiol.* *562*, 915–923.
41. van der Schaaf, A., and van Hateren, J.H. (1996). Modelling the power spectra of natural images: statistics and information. *Vision Res.* *36*, 2759–2770.
42. Girshick, A.R., Landy, M.S., and Simoncelli, E.P. (2011). Cardinal rules: visual orientation perception reflects knowledge of environmental statistics. *Nat. Neurosci.* *14*, 926–932.
43. Wallace, D.J., Greenberg, D.S., Sawinski, J., Rulla, S., Notaro, G., and Kerr, J.N.D. (2013). Rats maintain an overhead binocular field at the expense of constant fusion. *Nature* *498*, 65–69.
44. Tian, N. (2008). Synaptic activity, visual experience and the maturation of retinal synaptic circuitry. *J. Physiol.* *586*, 4347–4355.
45. Akimov, N.P., and Rentería, R.C. (2014). Dark rearing alters the normal development of spatiotemporal response properties but not of contrast detection threshold in mouse retinal ganglion cells. *Dev. Neurobiol.* *74*, 692–706.
46. Smith, G.B., Sederberg, A., Elyada, Y.M., Van Hooser, S.D., Kaschube, M., and Fitzpatrick, D. (2015). The development of cortical circuits for motion discrimination. *Nat. Neurosci.* *18*, 252–261.